

Rotational Isomerism of Ethanol and Matrix Isolation Infrared Spectroscopy

S. Coussan, Y. Bouteiller,[†] and J. P. Perchard*

Laboratoire de Spectrochimie Moléculaire, CNRS URA 508, Université Pierre et Marie Curie, Case Courrier 49, 4 Place Jussieu, 75252 Paris Cedex 05, France

W. Q. Zheng

LURE, Bâtiment 209D, Université Paris Sud, 91405 Orsay Cedex, France

Received: December 30, 1997; In Final Form: April 1, 1998

The vibrational spectrum of ethanol monomer trapped in argon and nitrogen matrices has been recorded in various conditions of temperature and irradiation. The structures and vibrational properties of the anti and gauche conformers have been investigated by ab initio calculations according to the DFT method. The comparison between observed and calculated frequencies allows an explanation of the matrix data and a proposal of a complete assignment for both conformers. The striking spectral changes observed in nitrogen matrices upon temperature cycling in the range 8–30 K are interpreted in term of anti \rightarrow gauche conversion. In contrast with these observations, the spectrum obtained in an argon matrix is insensitive to thermal effects, the anti form being the only one to be stabilized. Monochromatic irradiations in the OH and CO stretching regions were carried out with the purpose of inducing photorotamerization. In all cases only changes of trapping sites were observed, despite an interconversion barrier lower than the energy of the absorbed photons.

I. Introduction

In the course of a study of infrared induced interconversions between several forms of ethanol dimers trapped in inert matrices we were led to reexamine the vibrational spectrum of ethanol monomer. Noticeable spectral changes according to the nature of the matrix and to temperature cycling of highly diluted samples prompted us to consider the dependence of the vibrational properties with the conformation of the molecule.

The problem of rotational isomerism of ethanol has given rise to several spectroscopic studies in the microwave,^{1–3} infrared,^{4–12} and Raman^{13,14} domains. The presence of two conformers differing by the orientation of the OH bond with respect to the CCO plane has been clearly identified in microwave spectroscopy; the anti form (C_s symmetry) has been found to be slightly more stable than the gauche one (energy difference, 0.49 kJ mol⁻¹).³ Several rovibrational studies^{7,9,14} carried out on the OH stretching mode ($\nu(\text{OH})$) and its overtones ($n\nu(\text{OH})$) confirm the presence of the two conformers in the gas phase. The $\nu(\text{OH})$ frequency and the energy difference between the conformers were deduced from a thorough study of the overtones in the range 10 000–20 000 cm⁻¹ ($n = 3–6$).⁷ The anti form was found to be 2.9 kJ mol⁻¹ more stable than the gauche one, with a $\nu(\text{OH})$ frequency 16 ± 10 cm⁻¹ higher. This order was explained¹⁵ in terms of overlap between the lone pair orbital of the oxygen atom and the anti bonding σ^* orbital of the C–H bond for the anti structure. At last one will mention a short description by Barnes⁸ of the temperature dependence of the $\nu(\text{OH})$ absorption of ethanol trapped in solid nitrogen, interpreted in terms of anti/gauche thermal interconversion, without any further information about the other spectral domains.

On the other hand many quantum chemistry calculations were carried out on ethanol [see refs 10, 11, and 16, and references

cited therein]. Most of them deal with the relative stability of the conformers but, as discussed in refs 11 and 16, are not accurate enough to confidently predict even the sign of the energy difference. In two papers^{10,11} devoted to the vibrational optical activity of (*S*)-ethanol-1-*d*, valuable results about the vibrational spectra of both conformers have been obtained. These calculations are based on the scaled force field method combining experimental data and ab initio calculations.

The purpose of this paper is to show that the comparison between the spectra calculated according to the DFT technique for both conformers and the observed ones allows one to conclude that either one or the other species can be stabilized according to the nature of the matrix. Furthermore monochromatic irradiations in the CO and OH stretching regions offer the opportunity of studying photoisomerization involving the internal rotation of the hydroxyl group, as observed for nitrous acid^{17,18} and formic acid.¹⁹

II. Experimental Details

The matrix experiments were carried out in two laboratories, at Paris and Orsay, using two different devices. At Paris we used a closed cycle helium cryostat (Air Products CSW 202) coupled to a Bruker 120 interferometer and at Orsay a liquid helium cryostat (l'Air Liquide) coupled to a Mattson-Unicam Research series II interferometer. In both cases the gas mixtures were prepared by standard manometric technique and sprayed on a Ni or Au plated Cu block cooled to 17 K (N₂) or 20 K (Ar). The deposition rate was varied between 5 and 10 mmol h⁻¹. Irradiations in the 10 μm region were performed at Paris, with a homemade continuous wave (CW) CO₂ laser capable of delivering 200 mW on a selected emission line between 1092 and 1024 cm⁻¹. Irradiations in the 3 μm region were performed at Orsay using a homemade optical parametric oscillator (OPO) previously described in ref 20. The average power was 25 mW in the 3 μm region and the line width of the order of 1 cm⁻¹.

[†] Also at: Laboratoire de Physique des Lasers, Institut Galilée, Université Paris Nord, 93430 Villetaneuse, France.

TABLE 1: Geometrical Parameters (r , Å; α , deg) and Energy (hartrees) of the Anti and Gauche Conformers of Ethanol (Comparison with the Gas-Phase Data of the Anti Form²)

	anti		gauche
	calc	exp	
$r(\text{OH})$	0.9603	0.971	0.9611
$r(\text{CO})$	1.4319	1.431	1.4287
$r(\text{CC})$	1.5146	1.512	1.5212
$r(\text{CH})$ (methyl)	{ 1.0907 (ip) 1.0897 (op)}	1.088	1.0917; 1.0923; 1.0897
$r(\text{CH})$ (methylene)	1.0950	1.086	1.0952; 1.0892
$\alpha(\text{CCO})$	108.02	107.8	112.95
$\alpha(\text{COH})$	109.02	105.4	108.73
energy	-155.101 77		-155.101 61

Natural ethanol (Prolabo, RP grade) was dried over sodium and distilled under vacuum. Argon and nitrogen matrix gases (l'Air Liquide, 99.999%) were used without further purification.

III. Theoretical Calculations on Ethanol Monomer

Ab initio calculations have been carried out in the framework of the DFT theory, using the GAUSSIAN 92 computer code²¹ and the basis set 6-311++G(2d,2p) of Pople et al.²² Becke's three parameters functional²³ was used, including the gradient dependent exchange correction and the nonlocal correlation function of Lee, Yang, and Parr.²⁴

In a first step the full geometry optimization was carried out for the anti and gauche forms of ethanol. The former has C_s symmetry with distinguishable hydrogen atoms for the methyl group, one (ip) being in the plane symmetry, the two others (op) symmetrically located with respect to this plane. The most significant structural parameters are reported in Table 1 and compared to the experimental values of the anti form.²¹ The agreement is satisfactory except for the COH angle which is calculated 4° greater than observed. The results are also very close to those of previous calculations using post Hartree–Fock techniques.^{10,11} Some differences between the bond lengths of the anti and gauche structures are worth noting: $r(\text{OH})$ and $r(\text{CC})$ are shorter, but $r(\text{CO})$ is longer for anti than for gauche ethanol. As for the energy, it is found to be 0.42 kJ mol⁻¹ lower for the anti form than for the gauche form. This value is in remarkably good agreement with the one obtained by microwave spectroscopy.³

In a second step harmonic frequencies and infrared intensities of the 21 vibrational modes have been calculated. The 19 small-amplitude ones are reported in Tables 2 and 3 for the anti and gauche forms, respectively, together with an approximate description in terms of local symmetry coordinates. One shall note the complexity of the couplings between these coordinates for the modes in the range 1000–1350 cm⁻¹. No scaling factor was introduced in the frequency calculations, which renders difficult the comparison with the results of the previous calculations.^{10,11}

We have reported in Table 4 some significant frequency shifts between the two conformers which are the most useful for analyzing the matrix data. First the inequality $\nu(\text{OH})$ (anti) > $\nu(\text{OH})$ (gauche), which agrees with the gas-phase data,⁷ follows from the shortening of the O–H distance from the gauche to the anti form. In the same manner the mean shifts of the CH₂ and CH₃ stretching modes are correlated to changes in bond lengths—shortening and lengthening for CH₂ and CH₃, respectively, from anti to gauche. But the most noticeable conformation-induced spectral changes are located in the range 1000–1350 cm⁻¹. Their origin is mainly due to changes of couplings between the local symmetry coordinates, the corresponding force

TABLE 2: Comparison between Observed^a and Calculated Frequencies (cm⁻¹) of the Anti Conformer of C₂H₅OH

calc ^b	obs		approx descriptn
	Ar	N ₂	
3847.9 (29)	{ 3660.8 3655.6	(0.52) 3652.9	$\nu(\text{OH})$
3110.8 (32)	{ 2995.4 2992.4	(0.35) 2991.4	$\nu_a(\text{CH}_3)$ A''
3104.2 (28)	2984.6	(0.54) 2984.1	$\nu_a(\text{CH}_3)$
3042.0 (16)	2939.2	(0.15) { 2941.1 2935.9	$\nu_s(\text{CH}_3)$
3015.5 (45)	{ 2917.4 2912.9	(0.60) { 2909.6 2904.6	$\nu_a(\text{CH}_2)$ A''
2991.2 (65)	2899.6	(0.40) { 2893 2875.5 2867	$\nu_s(\text{CH}_2)$
1530.0 (1)	1487.0	(0.01) 1490.2	$\delta(\text{CH}_2)$
1505.1 (3)	1463.3	(0.06) 1463.5	$\delta_a(\text{CH}_3)$
1488.5 (6)	1445.0	(0.12) 1445.8	$\delta_a(\text{CH}_3)$ A''
1451.2 (11)	1416.3	(0.16) 1411.7	w(CH ₂)
1410.2 (1)	1371.5	(0.02) 1371.4	$\delta_s(\text{CH}_3)$
1300.7 (0)		1274.8	tw(CH ₂) A''
1271.3 (66)	1239.5	(1) 1256.3	$\delta(\text{OH})$
1178.0 (3)	1161.0	(0.04) { 1159.6 1139.9	$r(\text{CH}_2) + r(\text{CH}_3)$ A''
1095.4 (21)	{ 1091.7 1083.5 1076.9	(0.51) 1090.7	$\nu(\text{CCO}) + r(\text{CH}_3)$
1030.4 (70)	{ 1025.0 1016.4	(0.90) 1027.7	$\nu(\text{CCO}) + r(\text{CH}_3)$
894.7 (15)	{ 889.4 886.4	(0.17) 887.6	$\nu(\text{CCO})$
822.5(0)	811.8	(0.01)	$r(\text{CH}_2) + r(\text{CH}_3)$ A''
418.3(12)	416.5 ^c		$\delta(\text{CCO})$

^a Measurements at 9 K before annealing. In the case of a multiplet, the main component is in italics. Relative intensities between parentheses. ^b Intensities (km mol⁻¹) between parentheses. ^c Reference 6.

constants being only weakly dependent on the structure. The main point concerns the localization of a strong band at 1271 cm⁻¹ for anti ethanol, mainly assignable to the COH bending motion, without counterpart in the spectrum of the gauche form, this bending being shared among several modes in the range 1000–1400 cm⁻¹. One also shall note the presence of two modes between 1100 and 1000 cm⁻¹ for both conformers, around 1030 and 1090 cm⁻¹ for anti and 1070 and 1060 cm⁻¹ for gauche, which in both cases involve CCO skeleton stretching and CH₃ rocking motions. The corresponding bands form two doublets, which, as will be seen below, can be considered as fingerprints of the two conformers.

IV. Spectral Results

The spectral properties of ethanol trapped in solid nitrogen will be described first since they are the key for elucidating the conformational dependence of the vibrations of C₂H₅OH. Then the results obtained in argon will be considered in light of those in nitrogen. In all cases use of highly diluted samples (typically C₂H₅OH/matrix = 1/2000) makes negligible the effects of aggregation, even after temperature cycling up to 28 K in N₂ and 36 K in Ar.

N₂ Matrix. Typical annealing effect observed in the CO stretching region is displayed in Figure 1. Five bands at 1090.7, 1064.4–1063.0, 1058.1, and 1027.7 cm⁻¹ are observed after deposition. Annealing to 30 K causes the intensity decrease of those at 1090.7 and 1027.7 cm⁻¹, counterbalanced by the growth of the doublet 1064.4–1063.0 cm⁻¹ and of the weaker feature at 1058.1 cm⁻¹. Globally an intensity inversion upon annealing

TABLE 3: Comparison between Observed^a and Calculated Frequencies (cm⁻¹) of the Gauche Conformer of C₂H₅OH

gauche		approx descriptn
calc	obs N ₂	
3832.2 (23)	3649.5	<i>ν</i> (OH)
3106.6 (36)	2987.2	<i>ν</i> _a (CH ₃)
3092.9 (48)	{2984.5 2983.1}	<i>ν</i> _a (CH ₃)
3072.7 (5)	2951.9	<i>ν</i> _s (CH ₃)
3027.0 (16)	2929.7	<i>ν</i> _a (CH ₂)
3000.1 (59)	{2888.9 2886}	<i>ν</i> _s (CH ₂)
1521.4 (1)	1485.3	<i>δ</i> (CH ₂)
1498.0 (2)	1456.0	<i>δ</i> _a (CH ₃)
1493.8 (7)	{1453.1 1451.8}	<i>δ</i> _a (CH ₃)
1419.3 (37)	1389.1	w(CH ₂) + <i>δ</i> _s (CH ₃)
1407.1 (7)	1372.2	<i>δ</i> _s (CH ₃)
1373.1 (3)	1337.3	<i>δ</i> (OH) + w(CH ₂) + tw(CH ₂)
1282.6 (11)	1260.6	tw(CH ₂) + <i>δ</i> (OH)
1132.5 (5)	1125.8	<i>r</i> (CH ₂) + <i>r</i> (CH ₃)
1068.3 (103)	{1064.4 1063.0}	<i>ν</i> (CCO) + <i>δ</i> (OH)
1056.7 (26)	1058.1	<i>r</i> (CH ₃) + <i>δ</i> (OH)
881.4 (13)	{885.2 884.6}	<i>ν</i> (CCO) + <i>r</i> (CH ₃)
806.2 (3)	{812.1 811.3}	<i>r</i> (CH ₃) + <i>r</i> (CH ₂)
419.7 (11)		<i>δ</i> (CCO)

^a Measurements at 9 K after annealing of N₂ matrices. In the case of a multiplet, the main component is in italics. Relative intensities between parentheses. ^b Intensities (km mol⁻¹) between parentheses.

TABLE 4: Most Salient Spectral Differences^a between the Vibrational Spectra of Anti and Gauche Ethanol (Comparison between Calculated and Observed Values)

	calc	obs ^b	
$\Delta\nu$ (OH)	14.8	3.4; 16 ± 10 ^c	
$\Delta\bar{\nu}$ (CH ₂)	-33.1	-28.9	
$\Delta\bar{\nu}$ (CH ₃)	10.2	6.1	
<i>δ</i> (OH) anti	1271.3	1256.3	
modes in the 1100–1000 range	anti	[1095.4	1090.7
		[1030.4	1027.7
	gauche	[1068.3	1063.7
		[1056.7	1058.1

^a $\Delta\nu = \nu(\text{anti}) - \nu(\text{gauche})$; $\bar{\nu}$, mean values of the stretching modes. ^b N₂ matrix. ^c Reference 7.

is observed between two sets of bands in all the spectral regions. Comparison of these two sets with theoretical predictions (Tables 2 and 3) clearly shows that the set predominant before annealing has to be associated with the anti rotamer and the other to the gauche one. One shall note in particular the behavior of the modes involving the OH group. On one hand, after deposition, the *ν*(OH) mode is characterized by a doublet at 3652.9–3649.5 cm⁻¹, the high-frequency component being roughly three times stronger than the other. After annealing to 30 K the intensity of the 3652.9 cm⁻¹ becomes much weaker than the other. Its assignment to the anti form agrees with that proposed by Barnes⁸ and with the one deduced from the analysis of the *ν*(OH) overtones in the gas phase.⁷ On the other hand, the bending mode *δ*(OH) is associated after deposition to the strongest band of the whole spectrum at 1256.3 cm⁻¹, which nearly completely disappears after annealing. Its assignment to the conformer anti perfectly agrees with the theoretical predictions.

Ar Matrix. The spectral analysis in an argon matrix is readily carried out on the basis of the comparison with the data in solid nitrogen. Figure 2 displays the *ν*(CO) spectra of an

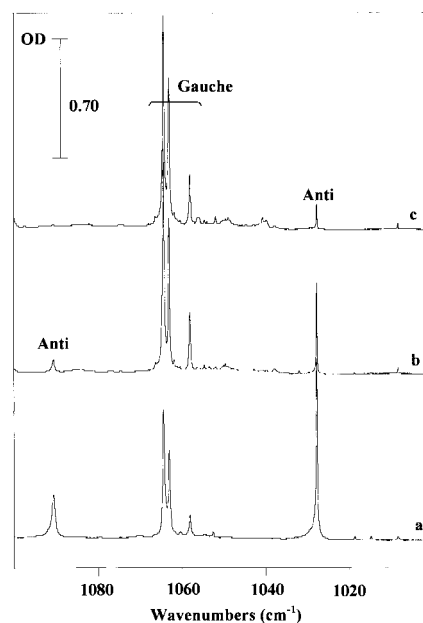


Figure 1. Evolution of the infrared spectrum of ethanol in solid nitrogen (1/1800) upon sample annealing. Spectra recorded at 8 K (a) after deposition, (b) after annealing to 28 K, and (c) after annealing to 30 K.

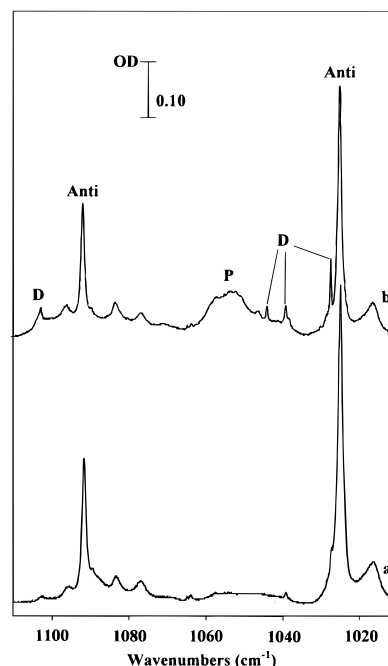


Figure 2. Evolution of the infrared spectrum of ethanol in solid argon (1/1800) upon sample annealing. Spectra recorded at 7 K (a) after deposition and (b) after annealing to 36 K. Note the intensity increase of the bands of (C₂H₅OH)₂ (D) and (C₂H₅OH)_n, n > 2 (P) after annealing.

Ar/C₂H₅OH = 2800 sample recorded before and after annealing to 36 K. No significant evolution—except some intensity increase of the bands around 1050 cm⁻¹ assignable to aggregates—is observed. In both cases two bands at 1091.8 and 1025.0 cm⁻¹ predominate, typical of anti ethanol. A very weak line at 1064.1 cm⁻¹, which does not significantly vary in intensity on annealing, probably arises from the gauche form. As for the *ν*(OH) and *δ*(OH) modes, they are respectively associated to a doublet at 3660.8–3655.6 cm⁻¹ and to a strong and narrow line at 1239.5 cm⁻¹. The whole spectrum is reported

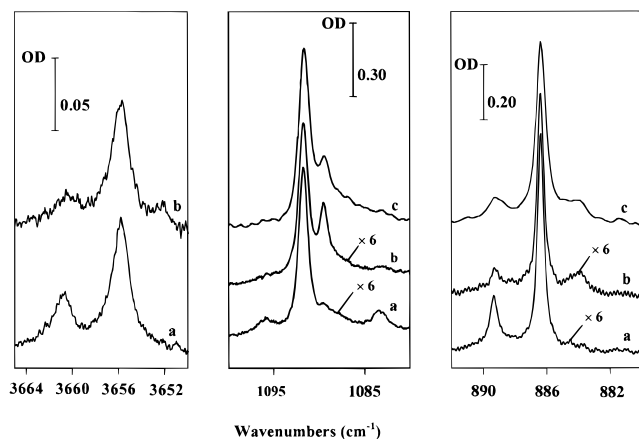


Figure 3. Effects of monochromatic irradiations on three bands of anti ethanol trapped in argon at 8 K. (a, b) $\text{C}_2\text{H}_5\text{OH}/\text{Ar} = 1/2800$, (a) before and (b) after 80 min irradiation at 1025.27 cm^{-1} ; (c) $\text{C}_2\text{H}_5\text{OH}/\text{Ar} = 1/350$, after 21 min irradiation at 3660.8 cm^{-1} .

in Table 2. It compares favorably with the one in N_2 assigned to anti ethanol.

V. Monochromatic Irradiations

Monochromatic irradiations in the 9.7 and $2.74\text{ }\mu\text{m}$ regions were carried out in order to induce rotamerization, as previously observed for some substituted ethanols.^{25–29} The experiments were conducted differently according to the wavelength. For irradiations in the $\nu(\text{CO})$ region we used an alternate procedure of irradiation/spectral recording and in the $\nu(\text{OH})$ region a permanent irradiation, the detector of the spectrometer being protected from the reflected OPO light by an interference filter transmitting in the range $500\text{--}1200\text{ cm}^{-1}$. Both methods proved equivalent, the lifetime of the species generated upon irradiations being much longer than the spectral recording duration in the temperature range $7\text{--}9\text{ K}$.

CO_2 Laser Irradiations. Argon Matrix. Positive effects have been obtained with the P(42) line at 1025.27 cm^{-1} . Spectra a and b of Figure 3 display some typical evolutions of the spectrum of anti ethanol. In the case where the absorption corresponding to one mode is split in several components, one of them is mainly affected by the irradiation and nearly totally disappears, with appearance of another absorption shifted by a few wavenumbers with respect to the parent component. The observed conversions are gathered in Table 5. The weakness of the shifts allows one to confidently conclude that the photoprocess corresponds to site interconversion and not to rotamerization. Incidentally the new sites are highly unstable, a temperature increase from 8 to 11 K for a few minutes regenerating the spectrum before irradiation.

Nitrogen Matrix. The same kind of observation as in solid argon has been made when irradiating the sample with the P(40) and R(40) lines at 1027.38 and 1090.04 cm^{-1} , respectively (Figure 4a,b and Table 5). These lines are in coincidence with strong absorptions of the anti conformer centered at 1027.7 and 1090.7 cm^{-1} . The appearance of new bands, shifted by less than 4 cm^{-1} from the parent ones, has to be interpreted in terms of site effect of anti ethanol, in the absence of any anti \rightarrow gauche rotamerization. The new sites are easily converted back to the previous ones by warming up the sample by a few kelvin.

OPO Irradiation. Argon Matrix. Positive effects have been observed upon irradiation at 3660.8 cm^{-1} , i.e., at the frequency of the weak high component of the $\nu(\text{OH})$ doublet. On one hand, for ethanol monomer, the spectral changes are identical to those obtained with the P(42) CO_2 laser line (Figure 3c) and

TABLE 5: Bands of Anti $\text{C}_2\text{H}_5\text{OH}$ Sensitive to Monochromatic Irradiations (ν_{irr}) and Frequencies (cm^{-1}) of the Metastable Sites Populated during These Irradiations

N_2 matrix		Ar matrix	
anti	ν_{irr}^a	metastable anti	metastable anti
2991.4		2993.1	3660.8
			2992.4
			2912.9
2904.6		2900.5	2901.3
1490.2		1489.4	
1463.5		1464.3	1463.7 (sh) ^b
1445.8		1446.6	1446.5 (sh)
1411.7		1413.4	
1371.4		1373.1	1370.4 (sh)
1256.3		1258.5	1239.2
1159.6		1161.0	
1090.7		1092.0	1096.1
			1091.9
			1083.5
1027.7		1028.4	1025.3
887.4		887.7	889.4
			815.1
			3652.2
			2995.8
			2917.4
			2899.7
			1462.5
			1444.1
			1371.3
			1238.1
			1089.5
			1023.8
			884.0
			812.1

^a $\nu_{\text{irr}} = 1027.38$ and 1090.04 cm^{-1} (P(40) and R(40) of CO_2) and 3652.9 cm^{-1} (OPO). ^b sh, shoulder to the main component. ^c $\nu_{\text{irr}} = 1025.27$ (P(42)) and 3660.8 cm^{-1} (OPO).

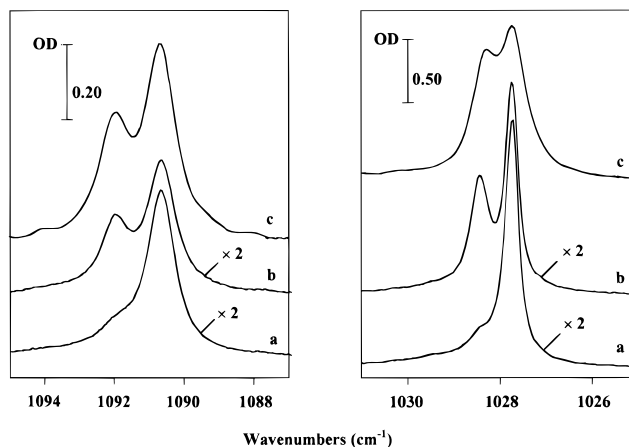


Figure 4. Effects of monochromatic irradiations on two bands of anti ethanol trapped in nitrogen at 8 K. (a, b) $\text{C}_2\text{H}_5\text{OH}/\text{N}_2 = 1/1300$, (a) before and (b) after 75 min irradiation at 1027.38 cm^{-1} ; (c) $\text{C}_2\text{H}_5\text{OH}/\text{N}_2 = 1/500$, after 15 min irradiation at 3652.9 cm^{-1} .

thus characterize site exchanges of anti ethanol and not rotamerization. On the other hand, noticeable spectral changes were obtained for the dimer. Indeed $(\text{C}_2\text{H}_5\text{OH})_2$ has an open chain structure, and the $\nu(\text{OH})$ frequency of the proton acceptor subunit is close to 3660 cm^{-1} . One thus concludes that irradiation at this frequency induces its isomerization, to be described in a forthcoming publication. Irradiation at 3655.6 cm^{-1} has also been carried out; the effects are identical, but much weaker than those observed at 3660.8 cm^{-1} .

Nitrogen Matrix. Irradiation at the frequency of the $\nu(\text{OH})$ band of anti ethanol at 3652.9 cm^{-1} induces the same effects as those obtained with the CO_2 laser lines (Figure 4c) while irradiation at the $\nu(\text{OH})$ frequency of the gauche form at 3649 cm^{-1} does not lead to significant spectral changes.

VI. Concluding Remarks

The purpose of the present study was the identification of the vibrational spectra of the anti and gauche forms of monomeric ethanol in view of a better understanding of those of the dimers. DFT as well as post HF calculations predict

noticeable spectral differences between anti and gauche conformers, suggesting the possibility of their unambiguous identification in inert matrices. Two experimental approaches were developed, on the basis of the hypotheses of thermal and infrared-induced interconversions. The quantum chemistry calculations remarkably support the hypothesis of an anti \rightarrow gauche conversion upon annealing of diluted nitrogen matrices; Barnes⁸ suggested that this conversion is reversible, which enables the trans/gauche energy difference to be deduced from the temperature dependence of the equilibrium constant. In our experiments the anti \rightarrow gauche conversion appeared to be irreversible; indeed we did not observe any spectral evolution when the sample was left for some hours in the dark in the temperature range 7–11 K after thermal conversion. We conclude thus that gauche ethanol is the stable form in this molecular matrix despite an energy higher than that of the anti form.^{3,7} In contrast anti ethanol is practically the only form observed in solid argon, whatever the thermal treatment of the sample. To our knowledge there is only one other example of inversion in the relative stability of conformers according to the matrix, namely, the hydrogen bonded methanol–water heterodimer in which the methanol molecule is proton donor in nitrogen and proton acceptor in argon. In this case it is also the thermodynamical stable form³⁰ which is stabilized in argon,³¹ and the higher energy one in nitrogen.³² But in both cases the energy difference is small, of the same order of magnitude as the matrix–dopant interaction. The stabilization of the gauche form in nitrogen should then be understood as arising from a decrease of the local energy of the doped matrix from anti to gauche ethanol. This energy can be written as the sum of dopant–nitrogen and nitrogen–nitrogen pair potentials involving the two or three first matrix shells surrounding the ethanol molecule. It includes in particular an electrostatic contribution which probably plays a predominant role for the stabilization of one conformer rather than the other.

The possibility of anti/gauche infrared photoconversion was examined by selectively exciting OH and CCO stretching modes. In contrast with the results on comparable systems such as halogeno ethanols^{25–29} and acids^{17–19} for which photorotamerization involving internal rotation around a single CO bond has been observed, no rotamerization has been identified in our experiments, the spectral changes being limited to small band splittings typical of site effects. The efficiency of the rotamerization process depends on the way the energy gained by excitation into a single mode redistributes among the vibrations. A simple scheme²⁶ is to consider that the transfer toward the levels associated with the reaction coordinate causes conversion, that toward other vibrational states energy randomization and dissipation to the matrix lattice. The absence of rotamerization after vibrational excitation of one conformer implies either the absence of energy transfer toward the highly excited $\tau(\text{OH})$ levels, in which the OH group behaves as a free rotor, or an internal vibrational energy redistribution (IVR) within this conformer. The first hypothesis requires the absence of coupling between the $\tau(\text{OH})$ and $\nu(\text{OH})$ or $\nu(\text{CCO})$ coordinates, which would be surprising in the light of the results obtained for nitrous and formic acids in which such couplings exist. The second hypothesis has to be examined in light of two specific properties of the ethanol molecule: it has two large amplitude/low-frequency torsional motions, $\tau(\text{OH})$ and $\tau(\text{CH}_3)$; it is characterized by a short characteristic time for energy redistribution from the OH stretch.^{33,34} It has been suggested³⁵ that the rate of IVR

could be increased by the presence of a methyl group in the molecule which increases the density of the level available for mixing. We thus suggest that the mixing involving the high-energy $\tau(\text{CH}_3)$ levels is more efficient than that involving the $\tau(\text{OH})$ ones so that redistribution occurs within the initially excited conformer. Such a difference in the behavior of the two torsional modes could be checked by studying the effect of monochromatic irradiation on the partially deuterated $\text{CH}_2\text{-DCH}_2\text{OH}$ species.

Acknowledgment. We thank Prof. F. Huisken for directing our attention on the conformational problem of ethanol and for providing a preprint of his work in press in *J. Phys. Chem.* We also thank C. Szopa and V. Vuitton for their technical assistance during their stay in this laboratory.

References and Notes

- (1) Michielsen-Effinger, J. *J. Mol. Spectrosc.* **1969**, *29*, 489.
- (2) Colot, J. P. Fourth Austin Symposium on Gas-Phase Molecular Structure, Austin, TX, 1972.
- (3) Kakar, R. K.; Quade, C. R. *J. Chem. Phys.* **1980**, *72*, 4300.
- (4) Oki, M.; Iwamura, H. *Bull. Chem. Soc. Jpn.* **1959**, *32*, 950.
- (5) Perchard J. P.; Josien, M. L. *J. Chim. Phys.* **1968**, *65*, 1834.
- (6) Barnes, A. J.; Hallam, H. E. *Trans. Faraday Soc.* **1970**, *66*, 1932.
- (7) Fang, H. L.; Swofford, R. L. *Chem. Phys. Lett.* **1984**, *105*, 5.
- (8) Barnes, A. J. *J. Mol. Struct.* **1984**, *113*, 161.
- (9) Van der Veken, B. J.; Coppens, P. *J. Mol. Struct.* **1986**, *142*, 359.
- (10) Dothe, H.; Lowe, M. A.; Alper, J. S. *J. Phys. Chem.* **1989**, *93*, 6632.
- (11) Shaw, R. A.; Wieser, H.; Dutler, R.; Rauk, A. *J. Am. Chem. Soc.* **1990**, *112*, 5401.
- (12) Ehbrecht, M.; Huisken, F. *J. Phys. Chem. A* **1997**, *101*, 7768.
- (13) Durig, J. R.; Bucy, W. E.; Wurrey, C. J.; Carreira, L. A. *J. Phys. Chem.* **1975**, *79*, 988.
- (14) Schiel, D.; Richter, W. *J. Chem. Phys.* **1983**, *78*, 6559.
- (15) Krueger, P. J.; Jan, J.; Wieser, H. *J. Mol. Struct.* **1970**, *5*, 375.
- (16) Bakke, J. M.; Bjerkeseth, L. H. *J. Mol. Struct.* **1997**, *407*, 27.
- (17) Baldeschwieler, J. D.; Pimentel, G. C. *J. Chem. Phys.* **1960**, *33*, 1008.
- (18) Mc Donald, P. A.; Shirk, J. S. *J. Chem. Phys.* **1982**, *77*, 2355.
- (19) Lundell, J. Private communication.
- (20) Coussan, S.; Loutellier, A.; Perchard, J. P.; Racine, S.; Peremans, A.; Tadjeddine, A.; Zheng, W. Q. *J. Chem. Phys.* **1997**, *107*, 6526.
- (21) Frish, M. J.; Trucks, G. W.; Schlegel, H. B.; Gill, P. M. W.; Johnson, B. G.; Wong, M. W.; Foresman, J. B.; Robb, M. A.; Head-Gordon, M.; Replogle, E. S.; Gompertes, R.; Andres, J. L.; Raghavachari, K.; Binkley, J. S.; Gonzalez, C.; Martin, R. L.; Fox, D. J.; Defrees, D. J.; Baker, J.; Stewart, J. J. P.; Pople, J. A. *GAUSSIAN 92/DFT*, Revision F.4; Gaussian, Pittsburgh, PA, 1993.
- (22) Krishnan, R.; Binkley, J. S.; Seeger, R.; Pople, J. A. *J. Chem. Phys.* **1980**, *72*, 650.
- (23) Frisch, M. J.; Pople, J. A.; Binkley, J. S. *J. Chem. Phys.* **1984**, *80*, 3265.
- (24) Becke, A. D. *J. Chem. Phys.* **1997**, *98*, 1053; **1993**, *98*, 5648.
- (25) Lee, C.; Wang, W.; Parr, R. G. *Phys. Rev. B* **1988**, *37*, 785.
- (26) Pourcin, J.; Davidovics, G.; Bodot, H.; Abouaf-Marguin, L.; Gauthier-Roy, B. *Chem. Phys. Lett.* **1980**, *74*, 147.
- (27) Hoffman, W. F., III; Shirk, J. S. *J. Chem. Phys.* **1985**, *89*, 1715.
- (28) Hoffman, W. F., III; Shirk, J. S. *J. Phys. Chem.* **1986**, *90*, 5706.
- (29) Hoffman, W. F., III; Shirk, J. S. *J. Mol. Struct.* **1987**, *157*, 275.
- (30) Kafafi, Z. H.; Marquardt, C. L.; Shirk, J. S. *J. Chem. Phys.* **1989**, *90*, 3087.
- (31) Stockman, P. A.; Blake, G. A.; Lovas, F. J.; Suenram, R. D. *J. Chem. Phys.* **1997**, *107*, 3782.
- (32) Bakkas, N.; Bouteiller, Y.; Loutellier, A.; Perchard, J. P.; Racine, S. *Chem. Phys. Lett.* **1995**, *232*, 90.
- (33) Bakkas, N.; Bouteiller, Y.; Loutellier, A.; Perchard, J. P.; Racine, S. *Chem. Phys.* **1993**, *99*, 3335.
- (34) Fraser, G. T.; Pate, B. H.; Bethardy, G. A.; Perry, D. S. *Chem. Phys.* **1993**, *175*, 223.
- (35) Heilweil, E. J.; Casassa, M. P.; Cavanagh, R. R.; Stephenson, J. C. *J. Chem. Phys.* **1986**, *85*, 5004.
- (36) Parmenter, C. S.; Stone, B. *J. Chem. Phys.* **1986**, *84*, 4710.